Self-assembly of T-shaped rod-coil block copolymer melts

Yingdong Xia, Jizhong Chen, Zhaoyan Sun, Tongfei Shi, Lijia An et al.

Citation: J. Chem. Phys. **131**, 144905 (2009); doi: 10.1063/1.3247192
View online: http://dx.doi.org/10.1063/1.3247192
View Table of Contents: http://jcp.aip.org/resource/1/JCPSA6/v131/i14
Published by the American Institute of Physics.

Self-assembly of T-shaped rod-coil block copolymer melts

Yingdong Xia (夏英东),[1] Jizhong Chen (陈继忠),[1,a)] Zhaoyan Sun (孙昭艳),[1] Tongfei Shi (石彤非),[1] Lijia An (安立佳),[1,b)] and Yuxi Jia (贾玉玺)[2]
[1]*State Key Laboratory of Polymer Physics and Chemistry, Changchun Institute of Applied Chemistry, Chinese Academy of Sciences, Changchun 130022, China*
[2]*School of Materials Science and Engineering, Shandong University, Jinan 250061, China*

(Received 24 April 2009; accepted 22 September 2009; published online 13 October 2009)

Self-assembled behavior of T-shaped rod-coil block copolymer melts is studied by applying self-consistent-field lattice techniques in three-dimensional space. Compared with rod-coil diblock copolymers with the anchor point positioned at one end, the copolymers with the anchor point at the middle of the rod exhibit significantly different phase behaviors. When the rod volume fraction is low, the steric hindrance of the lateral coils prevents the rods stacking into strip or micelle as that in rod-coil diblock copolymers. The competition between interfacial energy and entropy results in the formation of lamellar structures and the increasing thickness of the lamellar layer with increasing rod volume fraction. When the rod volume fraction is high, the graft density of the planar interface is decreased, which results in space-filling requirements and stretching penalty, thus leading to the stability of nonlamellar structures with curing interface. Furthermore, our results also suggest that the effect of the chain architecture on the self-assembled behavior is remarkable when the rod volume fraction is low, whereas the effect is weak when the rod volume fraction is high.
 [doi:10.1063/1.3247192]

I. INTRODUCTION

Rod-coil block copolymers are a family of materials that attract a lot of interest due to their fascinating ability to create supramolecular structures with well-defined shapes and functions.[1,2] For instance, self-assembly of these block copolymers could produce novel electronic, optoelectronic devices and biomimetic materials. In the past decades, various self-assembled morphologies such as lamellae, arrowhead lamellae, zigzag lamellae, wave lamellae, strips, honeycombs, hollow spherical, and cylindrical micelles have been observed for the rod-coil block copolymer systems.[2–5] The driving force responsible for the rich phase behavior arises from a combination of organizing forces including the mutual repulsion of the dissimilar blocks, the packing constraints imposed by the connectivity of each block, and the tendency of the rod block to form orientational order.

The self-assembled structure is in close relationship with the chain architecture, and therefore, one can design the architecture of the copolymer chain to explore various self-assembled structures and desired functions.[6] For example, by varying the number of blocks in rod-coil diblock copolymer or decorating the coil block with branches, many interesting phase behaviors have been observed.[7–9] Another means to design the rod-coil diblock copolymer is to move the anchor point from the rod end to the middle and a different rod-coil block copolymer with T-shaped architecture is obtained. This variation in the chain architecture is expected to affect the details of the molecular packing and thus the nature of thermodynamically stable self-assembled structures, which arouses people's interest both in experiments and simulations.[10–13] For example, Horch *et al.*[11] studied the self-assembled behavior of the T-shaped rod-coil block copolymers using Brownian dynamics in solution. They predicted stepped structures and two structurally different liquid crystalline bilayer phases. Later, Hong *et al.*[12,13] investigated the system with the method combing experiments and Brownian dynamics, and found interesting hierarchical structures. However, compared with rod-coil diblock copolymers, the studies on the T-shaped rod-coil block copolymer system are not so extensive that more efforts are needed to exploit it. In this paper, we implement the study of the self-assembled behavior of T-shaped rod-coil block copolymer melts using self-consistent-field theory (SCFT) lattice model[5] in three-dimensional space. Besides, the mesogen-jacketed liquid crystalline polymers (MJLCPs)[14] can be accessed by converting the T-shaped rod-coil block copolymers into a side chain polymer, and thus our findings are expected to shed some light on the research of the self-assembled behavior of MJLCPs.

Compared with block copolymers consisting of only flexible blocks, theoretical studies are less developed for rod-coil block copolymers due to the complicated entropy interactions that arise from the asymmetry between the two blocks and the tendency of the rod to orient itself parallel with the other rods. SCFT,[15] which has been proved to be a successful way to describe the phase behavior of traditional coil-coil block copolymers, has also been applied to rod-coil systems. One can use the Gaussian statistics to describe the flexible block, while using other theories to model the rigid section of the copolymer. For example, Matsen and Barrett[16] developed a rod-coil diblock copolymers' model, in which

a)Electronic mail: jzchen@ciac.jl.cn. Tel.: 86-431-85262137. FAX: 86-431-85262969.
b)Electronic mail: ljan@ciac.jl.cn. Tel.: 86-431-85262988. FAX: 86-431-85262126.

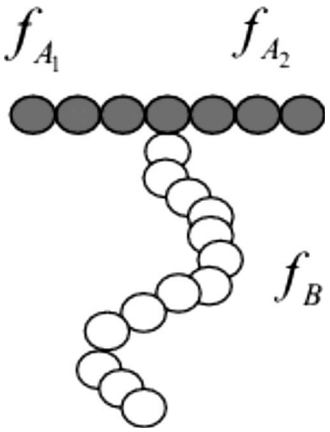

FIG. 1. Schematic illustration of the T-shaped block copolymer. The black (white) spheres indicate the rod (coil) segments.

they used Flory's lattice theory to account for orientational interactions between rods, but was restricted to one-dimensional smectic phases. Pryamitsyn and Ganesan[17] presented a SCFT model where the orientational interactions were included using Maier–Saupe interactions and predicted the phase diagram for rod-coil diblock copolymer for one and two dimensions. While other groups performed the simulation of rod-coil block copolymers without aligning interactions between the rigid blocks. Li and Gersappe[18] studied the phase diagram of rod-coil diblock copolymer by proposing a two dimensional SCFT lattice model where the chain rigidity was accounted by the rotational isomeric state scheme. In this paper, the SCFT lattice model is applied like our previous works,[5,7,8] and the rigid section of the copolymer is described similar to Li and Gersappe's method.

As shown in Fig. 1, the T-shaped rod-coil block copolymer is composed by a rod block with a laterally tethered coil block. f_{A_1} and f_{A_2} are used to denote the volume fraction of the two rod blocks besides the anchor point. We first consider the situation that the lengths of the two rod blocks are equal, i.e., $f_{A_1}=f_{A_2}$, and the phase diagram is constructed in f_{rod} versus χN to reveal the different phase behavior compared with that of rod-coil diblock copolymers with the anchor point at one end. Then we study the situation that the lengths of the two rod blocks are unequal, i.e., $f_{A_1}\neq f_{A_2}$, and a series of phase diagrams are constructed in f_{A_1}/f_{A_2} versus χN to understand how the chain architecture influence the self-assembled behavior with respect to different rod volume fractions.

II. THEORY

We consider a molten system of n T-shaped rod-coil block copolymers and the total degree of polymerization of each chain is N. As shown in Fig. 1, the chain is formed by three arms connected to the central point segment (anchor point), whose rodlike arm 1 and arm 2 are constrained to a linear structure with $f_{A_1}N$ and $f_{A_2}N$ segments of A, respectively, and flexible arm 3 is laterally tethered to the rod with f_BN segments of B. Therefore, the degree of polymerization of the T-shaped rod-coil block copolymer can be expressed as $N=f_{A_1}N+f_{A_2}N+f_BN+1$ (1 represents the anchor point). We suppose the segments of A block and B block have the same size and each segment occupies one lattice site, thus the total number of the lattice sites is $N_L=n(f_{A_1}N+f_{A_2}N+f_BN+1)$. For convenience, we use the segment size of block copolymer as the length unit. The transfer matrix depends only on the chain model used. For this system,[5] we assume that

$$\lambda_{r_{j,s}-r'_{j,s-1}}^{\alpha_{j,s}-\alpha'_{j,s-1}}=\begin{cases}1, & \alpha_{j,s}=\alpha'_{j,s-1},\\ 0, & \text{otherwise},\end{cases} \tag{1}$$

for the rod section and

$$\lambda_{r_{j,s}-r'_{j,s-1}}^{\alpha_{j,s}-\alpha'_{j,s-1}}=\begin{cases}0, & \alpha_{j,s}=-\alpha'_{j,s-1},\\ 1/(z-1), & \text{otherwise},\end{cases} \tag{2}$$

for the coil section which represents a self-avoiding chain. Here, $r_{j,s}$ and $\alpha_{j,s}$ denote the position and bond orientation of the sth segment of the jth copolymer, respectively. r' denotes the nearest neighboring site of r. α can be any of the allowed bond orientations depending on the lattice model used. We use the cubic lattice model which has six bond orientations and z is the coordination number of the lattice. We treat the branched molecule very similarly as our previous work.[8] The end segment distribution function $G^{\alpha_s}(r,s|1)$ that gives the statistical weight of all possible walks starting from segment 1, which may locate anywhere in the lattice, and ending at segment s ($s\leq f_jN, j=1,2,3$) at site r, is evaluated from the following recursive relation:

$$G^{\alpha_s}(r,s|1)=G(r,s)\sum_{r'_{s-1}}\sum_{\alpha'_{s-1}}\lambda_{r_s-r'_{s-1}}^{\alpha_s-\alpha'_{s-1}}G^{\alpha'_{s-1}}(r',s-1|1). \tag{3}$$

The initial condition is $G^{\alpha_1}(r,1|1)=G(r,1)$ for arms 1 and 3, and $G^{\alpha_1}(r,1|1)=G^{\alpha_1}(r,f_1N|1)\times G^{\alpha_1}(r,f_3N|1)/G(r,1)$ for arm 2. $G(r,s)$ is the free segment weighting factor and

$$G(r,s)=\begin{cases}\exp(-\omega_A(r_s)), & s\in A,\\ \exp(-\omega_B(r_s)), & s\in B.\end{cases}$$

Another end segment distribution function $G^{\alpha_s}(r,s|f_jN)$ ($j=1,2,3$) starting from the other arm end is evaluated from the following recursive relations:

$$G^{\alpha_s}(r,s|f_jN)=G(r,s)\sum_{r'_{s+1}}\sum_{\alpha'_{s+1}}\lambda_{r'_{s+1}-r_s}^{\alpha'_{s+1}-\alpha_s}G^{\alpha'_{s+1}}(r',s+1|f_jN) \tag{4}$$

with the initial conditions $G^{\alpha_1}(r,f_2N|f_2N)=G(r,f_2N)$ for arm 2 and

$$G^{\alpha_{f_jN}}(r,f_jN|f_jN)=\begin{cases}G^{\alpha_{f_2N}}(r,1|f_2N)G^{\alpha_{f_3N}}(r,f_3N|f_3N)/G(r,1), & j=1,\\ G^{\alpha_{f_2N}}(r,1|f_2N)G^{\alpha_{f_1N}}(r,f_1N|f_1N)/G(r,1), & j=3\end{cases}$$

for arms 1 and 3. The free energy function of F (in the unit of k_{BT}) can be expressed as[5]

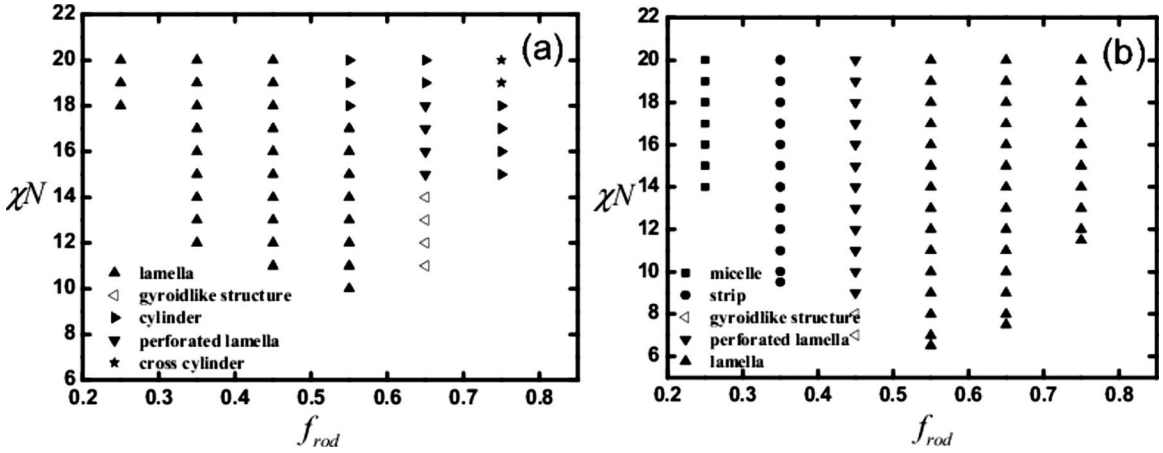

FIG. 2. Phase diagrams are shown for (a) the T-shaped rod-coil block copolymers ($f_{A_1}/f_{A_2}=1.0$) and (b) the rod-coil diblock copolymers (Ref. 8).

$$F=\sum_r\left\{\frac{\chi}{z}\sum_{r'}\phi_A(r)\phi_B(r')-\omega_A(r)\phi_A(r)-\omega_B(r)\phi_B(r)-\xi(r)[1-\phi_A(r)-\phi_B(r)]\right\}-n\ln Q, \tag{5}$$

where

$$Q=\frac{1}{N_L}\frac{1}{z}\sum_{r_N}\sum_{\alpha_N}G^{\alpha_1}(r,1|f_2N) \tag{6}$$

is the single chain partition function. Here, χ is the Flory–Hugginns interaction parameter which measures the incompatibility between A and B segments. $\phi_k(r)$ is the volume fraction field of block species k, which is independent of the individual polymer configuration, and $\omega_k(r)$ is the chemical potential field conjugated to $\phi_k(r)$. $\xi(r)$ is the potential field that ensures the incompressibility of the system, also known as a Lagrange multiplier. Minimizing the free energy function F with respect to $\phi_A(r)$, $\phi_B(r)$, $\omega_A(r)$, $\omega_B(r)$, and $\xi(r)$ leads to the following SCFT equations:

$$\omega_A(r)=\frac{\chi}{z}\sum_{r'}\phi_B(r')+\xi(r), \tag{7}$$

$$\omega_B(r)=\frac{\chi}{z}\sum_{r'}\phi_A(r')+\xi(r), \tag{8}$$

$$\phi_A(r)+\phi_B(r)=1, \tag{9}$$

$$\phi_A(r)=\frac{1}{N_L}\frac{1}{z}\frac{n}{Q}\sum_{s\in A}\sum_{\alpha_s}\sum_{j=1,2,3}\frac{G^{\alpha_s}(r,s|1)G^{\alpha_s}(r,s|f_jN)}{G(r,s)}, \tag{10}$$

$$\phi_B(r)=\frac{1}{N_L}\frac{1}{z}\frac{n}{Q}\sum_{s\in B}\sum_{\alpha_s}\sum_{j=1,2,3}\frac{G^{\alpha_s}(r,s|1)G^{\alpha_s}(r,s|f_jN)}{G(r,s)}. \tag{11}$$

In our calculations, the real space method is implemented to solve the SCF equations in a cubic lattice with periodic boundary conditions. To prevent bias of the resulting morphologies, our calculations are initiated with different random fields. The calculation stops when the free energy changes within a tolerance of 10^{-8}. The morphologies obtained correspond to either a stable or a metastable state. By comparing the free energy of the system, the relative stability of the morphologies can be assessed.

III. RESULTS AND DISCUSSION

In our studies, the ordered morphologies of the T-shaped rod-coil block copolymers depend on four tunable molecular parameters: f_{rod} (the volume fraction of the rod block), f_{A_1}/f_{A_2} (the ratio of volume fractions of rod blocks without the anchor point), χ (the Flory–Huggins interaction parameter depending on the temperature), and N (the total degree of polymerization of the block copolymer). The degree of polymerization is kept 20 the same as our previous work of rod-coil diblock copolymers[5] for comparison. Our calculations are preformed from $N_L=40^3$ to $N_L=80^3$ lattices to make sure that the emergences of the self-assembled structures are not constrained by the system size. Furthermore, our calculations are initiated with different random potentials to prevent bias of the resulting morphology. Below we present details on the simulation results.

We first study the polymer chain with symmetric structure that the two rod blocks besides the anchor point have an equal length, i.e., $f_{A_1}/f_{A_2}=1.0$. The phase diagram is constructed in f_{rod} versus χN, as shown in Fig. 2(a). To illustrate the effect of the changing architecture in the polymer chain on the self-assembled behavior, we also present the phase diagram of the rod-coil diblock copolymers[8] in Fig. 2(b) for comparison. Five stable morphologies are observed for the T-shaped rod-coil block copolymers in our simulations, including lamella, cylinder, cross cylinder, perforated lamella, and gyroidlike structure. It is obvious that regions of the stable structures for the T-shaped rod-coil block copolymers in the phase diagram are quite different from that of the rod-coil diblock copolymers.

For the low rod volume fractions ($f_{rod}\leq 0.55$), the lamellar structure dominates the majority of the phase diagram, which differs from that of rod-coil diblock copolymers where the nonlamellar structures are preferred, as shown in Fig. 2.

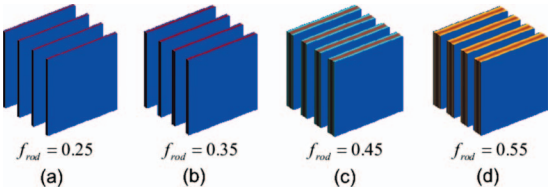

FIG. 3. Self-assembled lamellar structures (rod-rich) are shown for the T-shaped rod-coil block copolymers corresponding to rod volume fraction ranging from 0.25 to 0.55. The isosurface level is 0.5.

The variation in the self-assembled structures can be rationalized by considering the different characteristics of the two polymer chain architectures. When the anchor point is at the end of the rod, the rods trend to form strip or micelle structures.[5,19,20] For example, the rods in the strip structures present interdigited[5] or chiral[19] packing fashion for rod-coil diblock copolymers to reduce the elastic stretching energy of the coils. However, as the anchor point is moved to the middle of the rod, the rods cannot stack to such strip structures due to the steric hindrance caused by the laterally tethered coil blocks. To examine the rod orientation of the T-shaped rod-coil block copolymers in the lamellar structure, we carry out a further SCFT calculation as done in our previous work.[5] Similarly to the copolymer with the anchor point at the end of the rod, the rods of the T-shaped rod-coil block copolymers align along a common direction to maximize their contacts to minimize interfacial energy. Furthermore, the coils also attempt to maximize the free volume to maximize entropy. The competition between the interfacial energy and the entropy results in the fact that the lamellar structure is a stable morphology with respect to the T-shaped chain architecture, which is in good agreement with recent experiments and simulation results.[11,12]

Another interesting result observed in our simulation is that the thickness of the lamellar layer increases with the increase in the rod volume fraction, as shown in Fig. 3. In order to understand the formation of the different thickness of the lamellar layers, schematic representations of the packing fashion of the T-shaped rod-coil block copolymers are shown in Fig. 4. Compared with the copolymer with high rod volume fraction, the low rod volume fraction decreases the distance between the neighboring anchors of the T-shaped rod-coil block copolymers, leading to the formation of thin layers that allows the coils to adopt a less stretched conformation. When the rod volume fraction increases, the distance between the neighboring anchor points is increased, which lowers the grafting density at the rod-coil interface to increase the entropy. Meanwhile, more rod-rod contacts are required for the sake of lowering the interfacial energy. The

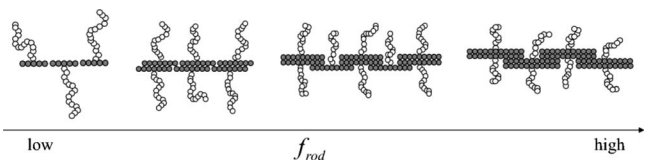

FIG. 4. Schematic representation of the packing fashion of the T-shaped rod-coil block copolymers in the lamellar structures with increasing rod volume fraction.

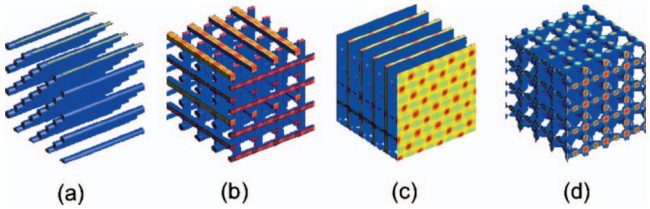

FIG. 5. Self-assembled structures (coil-rich) are shown for the T-shaped rod-coil block copolymer when $f_{rod} \geq 0.55$: (a) cylinder, (b) cross cylinder, (c) perforated lamella, and (d) gyroidlike structure. The isosurface level is 0.5.

interplay between the entropy and the interfacial energy induces the formation of thick layer lamellar structures. This result is qualitatively in agreement with the experimental work of Hong *et al.*[12] that the molecules based on a short rod self-assemble into thin sheets whereas the molecules based on a long rod self-assemble into thick sheets. However, the lamellar ordering of rods would confine rod-coil junctions to a flat interface, which results in a strong energetic penalty associated with low grafting density for high rod volume fractions. Furthermore, the coils are strongly stretched in thick layer lamellar structures as shown in Fig. 4, which is unfavorable for the entropy. As a result, the nonlamellar structures are more stable than the lamellar structures with the increase in the rod volume fraction.

For the high rod volume fractions ($f_{rod} \geq 0.55$), we observe the formation of nonlamellar structures with curving rod-coil interface including cylinder, cross cylinder, perforated lamella and gyroidlike structure (as shown in Fig. 5), which is again quite different from that of rod-coil diblock copolymers. For the rod-coil diblock copolymers, further increase in the rod volume fraction induces the formation of planar interface to decrease the interfacial energy as previously reported.[4,5,20] While for the T-shaped rod-coil block copolymers, as discussed above, the lamellar structure becomes unstable due to the space-filling requirements and the coil stretching. To lower the free energy, the planar rod-coil interface collapses and the curving interface is preferred. As shown in Fig. 2(a), the cylinder structure emerges when $0.55 \leq f_{rod} \leq 0.75$, which is formed by the coil blocks surrounded by continuous matrix of rods. Further calculations prove that the rods in the cylinder orient perpendicularly to the radial direction of the cylinder. When $f_{rod}=0.75$ and $\chi N \geq 19$, our simulation predicts a self-assembled structure not previously reported or predicted, denoted as cross cylinder [Fig. 5(b)], in which the cylinders can orient in three directions. Different simulation lattice sizes and random initial conditions confirm that this structure is robust and has the lowest free energy. For $f_{rod}=0.65$, the perforated lamella and the gyroidlike structure are observed, as shown in Figs. 5(c) and 5(d). The gyroidlike structure emerges above the order-disorder transition point, and the perforated lamella is formed with higher incompatibility of the rod and coil blocks.

Furthermore, in order to understand the effect of chain architecture on self-assembly of rod-coil block copolymers, we also gradually move the anchor point from the rod end to the middle, i.e., from a rod-coil diblock copolymer

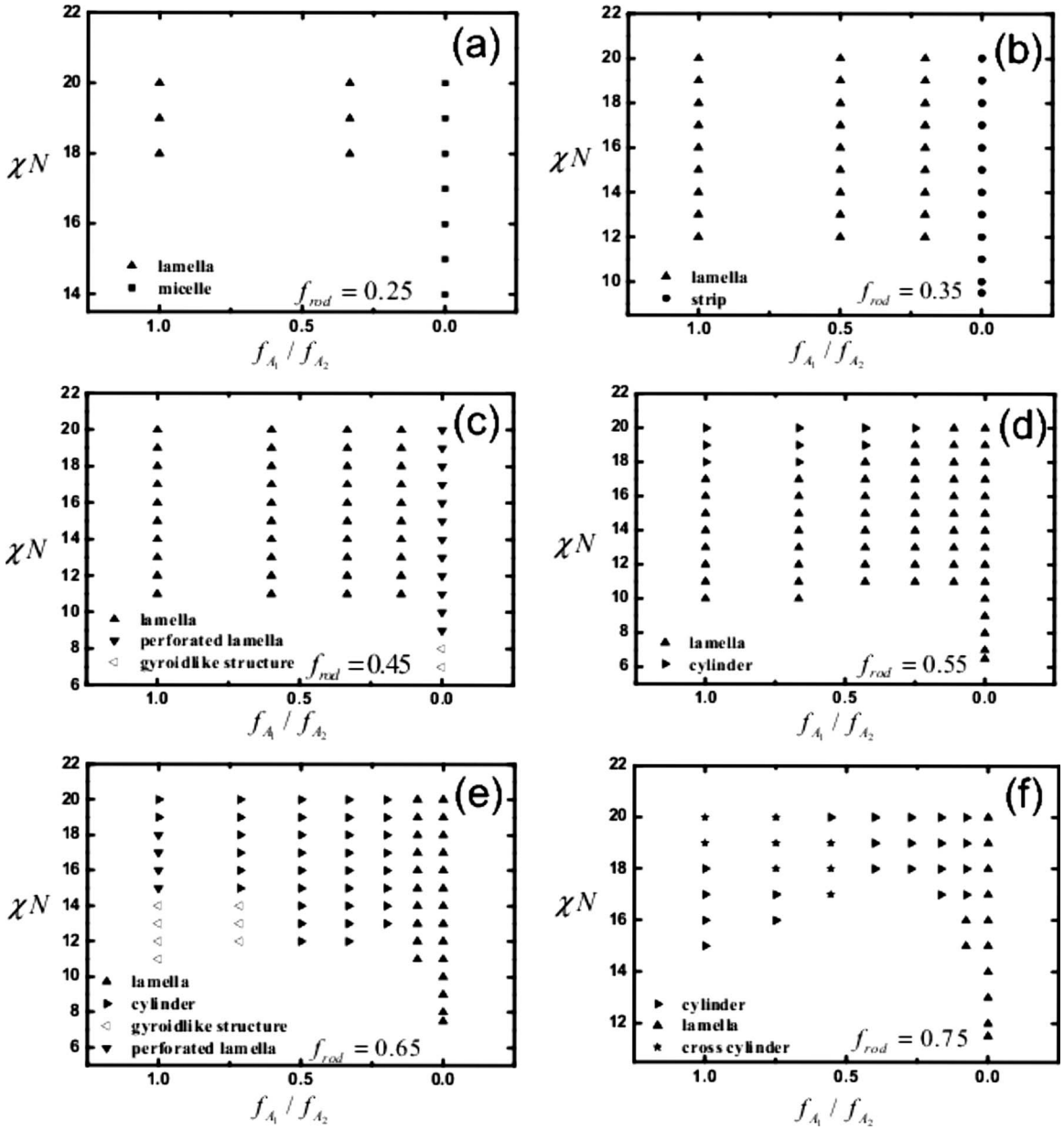

FIG. 6. Phase diagrams plotted in f_{A_1}/f_{A_2} vs χN with different rod volume fractions for (a) $f_{rod}=0.25$, (b) $f_{rod}=0.35$, (c) $f_{rod}=0.45$; (d) $f_{rod}=0.55$, (e) $f_{rod}=0.65$, and (f) $f_{rod}=0.75$.

($f_{A_1}/f_{A_2}=0.0$) to a T-shaped rod-coil block copolymer ($f_{A_1}/f_{A_2}=1.0$). The phase diagrams are constructed in f_{A_1}/f_{A_2} versus χN with respected to different rod volume fractions, as shown in Fig. 6. When the anchor point moves from the rod end to its closest segment, the rods encounter the anchor-induced hindrance to self-assemble the structures as that of rod-coil diblock copolymers. Especially when the coil volume fraction is high ($f_{rod}<0.55$), the hindrance becomes significant, which leads the self-assembled behavior of the rod-coil diblock copolymers suddenly changing to that of T-shaped ones [as shown in Figs. 6(a)–6(c)]. When the coil volume fraction is low ($f_{rod}\geq 0.55$), the hindrance is somewhat mitigated and the self-assembled behavior of the T-shaped rod-coil block copolymers emerges when the anchor point approaches the middle of the rod [as shown in Figs. 6(d)–6(f)].

IV. CONCLUSION

As an extension of our previous works, the self-assembled behavior of T-shaped rod-coil block copolymer melts is investigated by applying SCFT lattice techniques in three-dimensional space. Five stable morphologies are observed, i.e., lamella, cylinder, cross cylinder, perforated lamella, and gyroidlike structure. Compared with rod-coil diblock copolymers, the notable characteristic of the T-shaped rod-coil block copolymers is that the anchor point is at the middle of the rod, which imposes significant influence on the self-assembled behavior. For the low rod volume fractions, the lamellar structure is formed and the thickness of the lamellar layer increases with the increase in rod volume fraction, which is attributed to the interplay between the interfacial energy and the stretching entropy. For the high rod

volume fractions, the graft density of the planar interface is decreased and thus the lamellar structure encounters space-filling requirements and stretching penalty of the coil, which lead to the formation of nonlamellar structures with curving interface. Moreover, the self-assembled behavior of the T-shaped rod-coil block copolymers emerges when $f_{A_1}/f_{A_2} > 0$ for the low rod volume fractions and $f_{A_1}/f_{A_2} \approx 1$ for the high rod volume fractions.

Our model and results should encourage the search for the phase behavior of MJLCPs, for the T-shaped rod-coil block copolymer can be viewed as a unit of a MJLCP.[14] The MJLCPs are a new type of rod-coil block copolymer, which exhibits rich self-assembly characteristics and potential use in functional materials. By applying our lattice self-consistent field model, tuning the parameters that affect the self-assembly morphologies, such as the molecular weight, the volume and shape effects of mosogenic units, the architecture of the polymer chain, etc, the self-assembled behavior of MJLCPs are expected to be explored in three-dimensional space.

ACKNOWLEDGMENTS

This work was supported by the National Natural Science Foundation of China (Grant Nos. 20804047, 20574070, 20774096, and 20734003) Programs and the Fund for Creative Research Groups (Grant No. 50621302), and subsidized by the Special Funds for National Basic Research Program of China (Grant No. 2005CB623800).

[1] J. M. Lehn, *Supramolecular Chemistry* (VCH, Weinheim, 1995); S. I. Stupp, V. LeBonheur, K. Walker, L. S. Li, K. E. Huggins, M. Keser, and A. Amstutz, Science **276**, 384 (1997); R. Osterbacka, C. P. An, X. M. Jiang, and Z. V. Vardeny, *ibid.* **287**, 839 (2000).
[2] M. Lee, B. K. Cho, and W. C. Zin, Chem. Rev. (Washington, D.C.) **101**, 3869 (2001).
[3] J. T. Chen, E. L. Thomas, C. K. Ober, and S. S. Hwang, Macromolecules **28**, 1688 (1995); L. H. Radzilowski, B. O. Carragher, and S. I. Stupp, *ibid.* **30**, 2110 (1997); N. K. Oh, W. C. Zin, J. Hwan, and M. Lee, Polymer **47**, 5275 (2006); M. Lee, B. K. Cho, K. Ihn, W. K. Lee, N. K. Oh, and W. C. Zin, J. Am. Chem. Soc. **123**, 4647 (2001).
[4] J. T. Chen, E. L. Thomas, C. K. Ober, and G.-P. Mao, Science **273**, 343 (1996).
[5] J. Z. Chen, C. X. Zhang, Z. Y. Sun, Y. S. Zheng, and L. J. An, J. Chem. Phys. **124**, 104907 (2006).
[6] J. H. Ryu and M. Lee, Struct. Bonding (Berlin) **128**, 63 (2008).
[7] J. Z. Chen, C. X. Zhang, Z. Y. Sun, L. J. An, and Z. Tong, J. Chem. Phys. **127**, 024105 (2007); J. Z. Chen, Z. Y. Sun, C. X. Zhang, L. J. An, and Z. Tong, *ibid.* **128**, 074904 (2008).
[8] Y. D. Xia, Z. Y. Sun, T. F. Shi, J. Z. Chen, and L. J. An, Polymer **49**, 5596 (2008).
[9] M. U. Pralle, C. M. Whitaker, P. V. Braun, and S. I. Stupp, Macromolecules **33**, 3550 (2000); G. N. Tew, M. U. Pralle, and S. I. Stupp, Angew. Chem. Int., Ed. **39**, 517 (2000).
[10] K. H. Kim, J. Huh, and W. H. Jo, Macromolecules **37**, 676 (2004).
[11] M. A. Horsch, Z. L. Zhang, and C. S. Glotzer, Nano Lett. **6**, 2406 (2006).
[12] D. J. Hong, E. Lee, and M. Lee, J. Am. Chem. Soc. **130**, 14448 (2008).
[13] D. J. Hong, S. C. Glotzer, and M. Lee, Angew. Chem., Int. Ed. **48**, 1664 (2009).
[14] Y. F. Zhao, X. H. Fan, X. H. Wan, and X. F. Chen, Macromolecules **39**, 948 (2006); C. Y. Li, K. K. Tenneti, and D. Zhang, *ibid.* **37**, 2854 (2004).
[15] M. W. Matsen and M. Schick, Phys. Rev. Lett. **72**, 2660 (1994).
[16] M. W. Matsen and C. Barrett, J. Chem. Phys. **109**, 4108 (1998).
[17] V. Pryamitsyn and V. Ganesan, J. Chem. Phys. **120**, 5824 (2004).
[18] W. T. Li and D. Gersappe, Macromolecules **34**, 6783 (2001).
[19] M. A. Horsch, Z. L. Zhang, and S. C. Glotzer, Phys. Rev. Lett. **95**, 056105 (2005).
[20] B. D. Olsen and R. A. Segalman, Macromolecules **40**, 6922 (2007); M. Reenders and G. ten Brinke, *ibid.* **35**, 3266 (2002).